Molecular basis for discrimination of cGAMP linkage isomers by a c-di-GMP-II riboswitch variant

Xiaochen Xu[1,†], Wang Cheng[2,†], Huiqin You[1], Zejia Hu[1], Xinyue Bao[1], Hongcheng Li[1], Jinzhu Zhang[1], Dinshaw J. Patel[2,*] and Aiming Ren[1,*]

[1] Department of Cardiology of The Second Affiliated Hospital and Life Sciences Institute and School of Medicine, Zhejiang University, Hangzhou 310058, China

[2] Structural Biology Program, Memorial Sloan-Kettering Center, New York, New York 10065, USA.

[†]The first two authors should be regarded as Joint First Authors.

*To whom correspondence should be addressed.

Email: aimingren@zju.edu.cn and pateld@mskcc.org

RNA is emerging as a prominent therapeutic target, raising a fundamental question of how RNA molecules specifically recognize small molecules with highly similar chemical structures. Riboswitches, conserved regulatory RNA elements located in the 5' UTRs of mRNAs, directly bind metabolites and regulate downstream gene expression through ligand-induced conformational changes, thereby playing critical roles in maintaining cellular homeostasis (1-3). The diverse ligand-recognition strategies employed by riboswitches provide an excellent model system for investigating the molecular principles underlying RNA–small molecule recognition.

Cyclic dinucleotides are essential second messengers that mediate cellular responses to environmental stimuli (4). Four classes of cyclic dinucleotide-responsive riboswitches have been identified, including c-di-GMP-I/II riboswitch, c-di-AMP riboswitch and 3',3'-cGAMP riboswitch, which are involved in involved in cyclic dinucleotide synthesis, degradation, and signaling (5-9). 2′,3′-cGAMP is a linkage isomer of 3′,3′-cGAMP, differing in phosphodiester connectivity. As a well-established second messenger, it triggers mammalian innate immune responses (10) and induces membrane shearing and promotes broad antiphage immunity in bacteria (11). However, a natural 2',3'-cGAMP-responsive riboswitch has not yet been identified. A 2′,3′-cGAMP-binding riboswitch variant, termed BhP1-5delC aptamer, was generated through mutational analysis of a c-di-GMP-II riboswitch from *Bacillus halodurans* C-125 with a single nucleotide deletion (12).

To investigate the specific recognition of 2′,3′-cGAMP and its linkage isomer 3′,3′-cGAMP by RNA, we determined the crystal structures of BhP1-5delC in complex with each ligand, respectively. Unexpectedly, the two ligands adopt inverted orientations within the same binding pockets. Combined with structural analysis and mutational assays, these results elucidate the molecular basis underlying RNA-mediated discrimination of cyclic dinucleotides and their linkage isomers, highlighting the remarkable sensitivity of RNA binding pockets to subtle structural variations and provides a mechanistic framework for understanding ligand specificity in RNA–small molecule recognition.

Results

The tertiary structures of BhP1-5delC in complex with 2',3'-cGAMP and 3',3'-cGAMP (Fig. 1*A-D*) closely resemble that of the c-di-GMP-II riboswitch(13). The RNA adopts a three-helical junctional scaffold that constituted by stem P1, P2 and the pseudoknot stem P4. Stem P3 spans the overall fold, linking stem P2 and P4 as a helix bridge.

All three ligands adopt a "C"-shape conformation and bind within the three-way junction in a nearly identical manner. The ribose-phosphate backbone of ligand stacks against the first A–U base pair of stem P2, while the nucleobases are positioned between stems P1 and P4 (Fig. 1*E, I*). An adenine from P4 forms the ceiling of the binding pocket, and a noncanonical base pair of stem P1, A•G in BhP1-5delC, defines the bottom of the pocket. Within the pocket, the upper nucleobase of ligand is recognized by another adenine from P4, while the lower nucleobase interacts with a guanine from P4. Besides, a third adenine from P4 is intercalated between the two bases of ligands.

A detailed comparison of the two binding pockets reveals a prominent difference at the lateral surface. The A–U base pair adjacent to the ligand phosphodiester backbone forms a canonical Watson-Crick base pair in 2',3'-cGAMP-bound state. In contrast, the deflecting bases of A and U form only one hydrogen bond in 3',3'-cGAMP-bound state (Fig. 1*E, I*).

Another notable difference is the reversed orientation of the ligand bases in the 2',3'-cGAMP and 3',3'-cGAMP complexes. In 2',3'-cGAMP-bound structure, GMP occupies the upper position, stacking between A56 and A65. Its 1-NH and 2-NH_2 form three hydrogen bonds with the sugar edge of A64, thereby designated G_α (Fig. 1*G*). The AMP moiety (A_β) resides at the lower position, stacking between A65 and A8. Its 6-NH_2 forms one hydrogen bond and its N1 forms two hydrogen bonds with the Watson-Crick edge of G68, mediated by one water (Fig. 1*H*). In contrast, in 3',3'-cGAMP-bound structure, AMP occupies the upper position between A56 and A65, whereas GMP is located at the lower position between A65 and A8, and are thus designated A_α and G_β, respectively. A_α interacts with A64, forming two hydrogen bonds with the sugar edge of

A64 via its 6-NH_2 and N1 (Fig. 1*K*). G_β is recognized by 68G, with its 1-NH and 2-NH_2 each forming one hydrogen bond with O6 of G68 directly, without involvement of water or metal ions (Fig. 4*L*).

Given that a key difference between the two ligand-binding pockets lies in the A9-U55 base pair in stem P2 (Fig. 2*A*, *B*), we introduced a G-C base pair to replace A-U pair, generating the A9G/U55C mutant to evaluate its impact on the ligand-binding selectivity. We first determined the structures of BhP1-5delC-A9G/U55C in complex with 2',3'-cGAMP and 3',3'-cGAMP, respectively, and found that the introduced A9G and U55C mutations form a canonical Watson–Crick base pair in both ligand-bound states (Fig. 2*C*, *D*). The orientations of the two bound ligands, 2',3'-cGAMP and 3',3'-cGAMP remain unchanged relative to the wild-type RNA. Moreover, the direct hydrogen-bonding interactions, as well as the involved binding-pocket residues are highly similar between the wild-type and A9G/U55C mutant complexes (Fig. 2*C*, *D*). However, isothermal titration calorimetry (ITC) titration revealed that the A9G/U55C mutant exhibits increased binding affinity for 2',3'-cGAMP (K_d decreased from 460 nM to 139 nM), while its binding affinity for 3',3'-cGAMP is reduced (K_d increased from 11.4 nM to 33.4 nM). As a result, the selectivity gap between 3',3'-cGAMP and 2',3'-cGAMP recognition is reduced from 41.8-fold to 4.2-fold (Fig. 2*E*, *F*).

Discussion

In this study, we determined the structures of the BhP1-5delC aptamer, derived from the c-di-GMP-II riboswitch, in complex with either 2',3'-cGAMP or 3',3'-cGAMP. Although recent advances in artificial intelligence have significantly improved biomacromolecular structure prediction, widely used tools such as AlphaFold remain limited in RNA structure prediction, largely due to the relatively sparse availability of high-resolution RNA structural data. We compared our experimentally determined structure with the predicted model of BhP1-5delC bound to 2',3'-cGAMP. While the overall RNA architectures are broadly consistent, the ligand orientation is reversed, and the position of its nucleobases is shifted between the predicted and experimentally

determined structures. In addition, the key residues forming the binding pocket, such as A56, adopt markedly different local conformations, resulting in incorrect hydrogen-bonding interactions between the RNA and ligand nucleobases in the predicted model. Such fine structural details remain difficult to predict at present, while they are essential to understand the molecular basis underlying ligand discrimination by RNA.

Our structural analyses uncover distinct architectural features and ligand-binding pockets that define the molecular basis of BhP1-5delC discrimination among cyclic dinucleotides. These results reveal how RNA achieves selective recognition of cyclic dinucleotide linkage isomers and provide a framework for identifying previously unrecognized 2',3'-cGAMP-responsive riboswitches within existing c-di-GMP-II riboswitch databases and broader RNA sequence repositories. Importantly, cyclic dinucleotides are pivotal cellular signaling molecules that play critical roles in diverse biological processes. Our results highlight the broader biological relevance of RNA-mediated recognition of small signaling molecules and underscore RNA as an attractive and versatile target for small-molecule drug discovery. More broadly, this study provides a significant structural and mechanistic reference for understanding RNA-small molecule recognition principles, offering a framework that may guide the identification and design of RNA-targeting ligands in future chemical biology and therapeutic applications.

Materials and Methods

All RNAs were generated by in vitro transcription method. The cyclic dinucleotide ligands 2',3'-cGAMP and 3',3'-cGAMP were purchased commercially. For crystallization, RNAs were refolded in the presence of ligand and crystallized by sitting-drop vapor diffusion at 16 °C. Structures were determined by molecular replacement. Data collection and refinement statistics are provided in *Dataset_S01*. All RNA-ligand binding constants and thermodynamic parameters from ITC experiments are summarized in *Dataset_S02*. Additional experimental procedures, construct information, and crystallization conditions are described in the *SI Appendix*.

Data, Materials, and Software Availability

Atomic coordinates and structure factors for the reported crystal structures have been deposited with the Protein Data Bank (www.rcsb.org) under accession numbers 22MT (BhP1-5delC with 2',3'-cGAMP), 22MX (BhP1-5delC_A9G/U55C with 2',3'-cGAMP), 22MZ (BhP1-5delC with 3',3'-cGAMP), 22MW (BhP1-5delC_A9G/U55C with 3',3'-cGAMP) respectively. All study data are included in the article and/or *SI Appendix*.

Acknowledgments

This work was supported by the National Natural Science Foundation of China [32325029 to A.R., 32401070 to X.X.], Zhejiang Provincial Natural Science Foundation of China [LD25C050002 to A.R.], and the National Key Research and Development Project of China [2023YFC2604300 to A.R.]. Funding to pay the Open Access publication charges for this article was provided by Zhejiang University. We thank the staff members of the Large-scale Protein Preparation System, BL-17B, BL-17U1, BL18U1, BL-19U1, and BL02U1 beamlines at the National Facility for Protein Science in Shanghai (NFPS), Zhangjiang Lab, China for providing technical support and assistance in data collection and analysis.

Author contributions

X.X., W.C., A.R., and D.J. designed research; X.X., W.C., H.Q., Z.H., X.B., and H.L. performed research; X.X., W.C., A.R., J.Z., and D.J. analyzed data; and X.X., A.R., and D.J. wrote the paper.

Competing interests

The authors declare no competing interest.

Supporting Information

Appendix 01 (PDF)

Dataset_S01 (XLSX), Dataset_S02 (XLSX)

References

1. A. D. Garst, A. L. Edwards, R. T. Batey, Riboswitches: structures and mechanisms. *Cold Spring Harbor perspectives in biology* **3** (2011).
2. R. R. Breaker, Riboswitches and the RNA world. *Cold Spring Harbor perspectives in biology* **4** (2012).
3. A. Serganov, E. Nudler, A decade of riboswitches. *Cell* **152**, 17-24 (2013).
4. P. Aline Dias da, A. Nathalia Marins de, A. Gabriel Guarany de, S. Robson Francisco de, G. Cristiane Rodrigues, The World of Cyclic Dinucleotides in Bacterial Behavior. *Molecules* **25** (2020).
5. N. Sudarsan *et al.*, Riboswitches in eubacteria sense the second messenger cyclic di-GMP. *Science* **321**, 411-413 (2008).
6. E. R. Lee, J. L. Baker, Z. Weinberg, N. Sudarsan, R. R. Breaker, An allosteric self-splicing ribozyme triggered by a bacterial second messenger. *Science* **329**, 845-848 (2010).
7. J. W. Nelson *et al.*, Riboswitches in eubacteria sense the second messenger c-di-AMP. *Nature chemical biology* **9**, 834-839 (2013).
8. J. W. Nelson *et al.*, Control of bacterial exoelectrogenesis by c-AMP-GMP. *Proceedings of the National Academy of Sciences of the United States of America* **112**, 5389-5394 (2015).
9. C. A. Kellenberger *et al.*, GEMM-I riboswitches from Geobacter sense the bacterial second messenger cyclic AMP-GMP. *Proc Natl Acad Sci U S A* **112**, 5383-5388 (2015).
10. J. Wu, Z. J. Chen, Innate immune sensing and signaling of cytosolic nucleic acids. *Annu Rev Immunol* **32**, 461-488 (2014).
11. Y. Gao *et al.*, 2'3'-cGAMP-induced membrane shearing promotes broad antiphage immunity. *Cell* 10.1016/j.cell.2026.03.043 (2026).
12. D. Bose, Y. Su, A. Marcus, D. H. Raulet, M. C. Hammond, An RNA-Based Fluorescent Biosensor for High-Throughput Analysis of the cGAS-cGAMP-STING Pathway. *Cell chemical biology* **23**, 1539-1549 (2016).
13. K. D. Smith, C. A. Shanahan, E. L. Moore, A. C. Simon, S. A. Strobel, Structural basis of differential ligand recognition by two classes of bis-(3'-5')-cyclic dimeric guanosine monophosphate-binding riboswitches. *Proceedings of the National Academy of Sciences of the United States of America* **108**, 7757-7762 (2011).

Figure captions

Fig.1. Structure of BhP1-5delC in complex with 2',3'-cGAMP and 3',3'-cGAMP. ***(A)*** Secondary structure of BhP1-5delC. ***(B and C)*** Chemical structure of 2',3'-cGAMP and 3',3'-cGAMP. ***(D)*** Schematic representation of the tertiary structure of BhP1-5delC. ***(E)*** The binding pocket of BhP1-5delC bound with 2',3'-cGAMP**.** ***(F)*** Close-up view of the base pair A9-U55 in 2',3'-cGAMP-bound state. ***(G)*** A64 forms three hydrogen bonds with G_{α} of 2',3'-cGAMP. ***(H)*** A_{β} of 2',3'-cGAMP is recognized by G68. ***(I)*** The binding pocket of BhP1-5delC bound with 3',3'-cGAMP**.** ***(J)*** Close-up view of the base pair A9-U55 in 3',3'-cGAMP-bound state. ***(K)*** The A_{α} of 3',3'-cGAMP is interacted with A64 through two hydrogen bonds.

Fig.2. Comparison of binding pockets underlying ligand discrimination. ***(A-D)*** Binding pockets of BhP1-5delC and BhP1-5delC-A9G/U55C mutant in complex with 2',3'-cGAMP and 3',3'-cGAMP, respectively. ***(A)*** BhP1-5delC bound to 2',3'-cGAMP. ***(B)*** BhP1-5delC bound to 3',3'-cGAMP. ***(C)*** BhP1-5delC-A9C/U55G bound to 2',3'-cGAMP. (D*)* BhP1-5delC-A9C/U55G bound to 3',3'-cGAMP. ***(E,F)*** Overlay of ITC titration heat plots of BhP1-5delC and mutant A9G/U55C titrated with 2',3'-cGAMP and 3',3'-cGAMP, respectively.

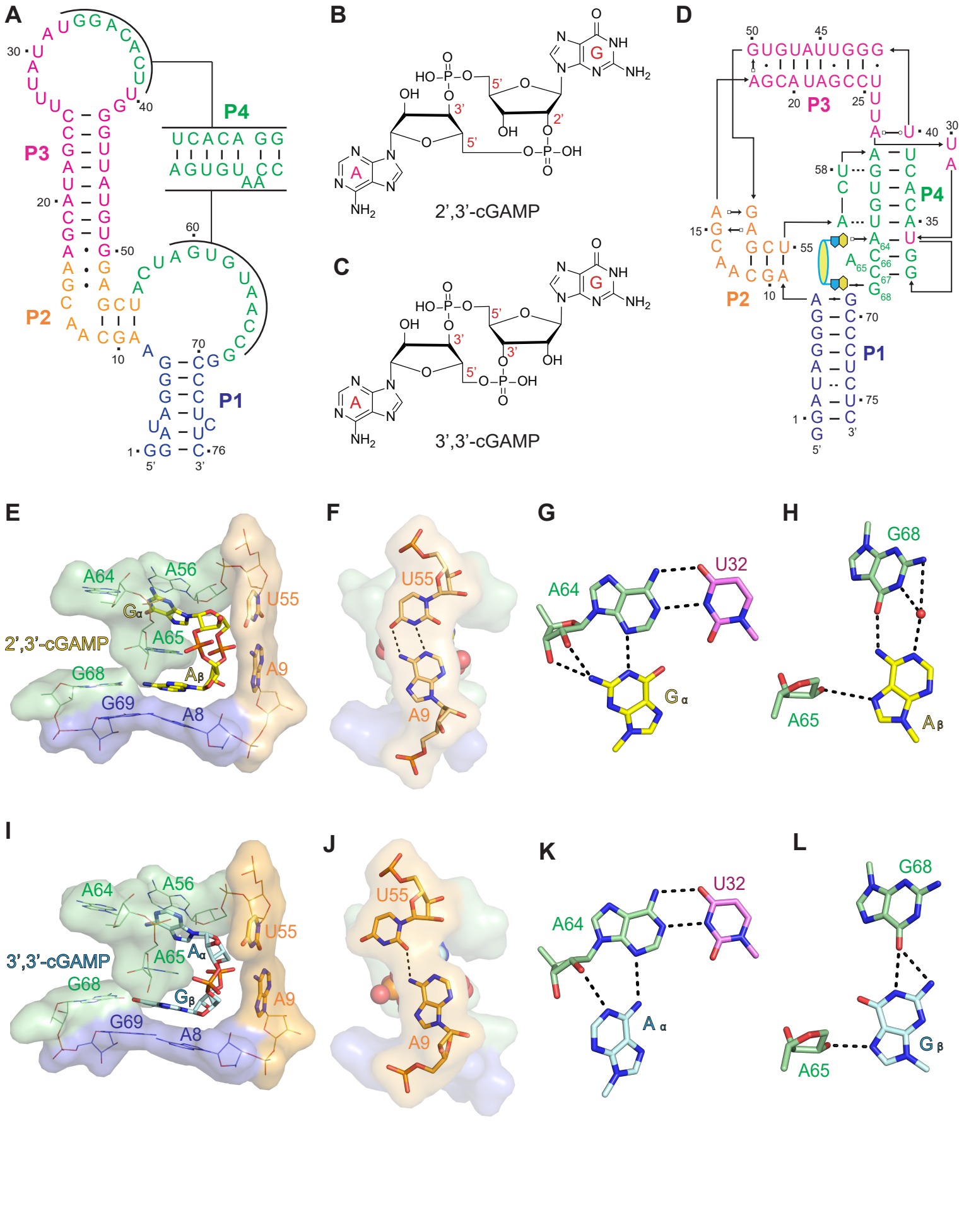
A
P4
P3
P2
P1
B
2',3'-cGAMP
C
3',3'-cGAMP
D
P3
P4
P2
P1
E
2',3'-cGAMP
A64
A56
U55
A65
G68
G69
A8
A9
F
U55
A9
G
A64
U32
H
G68
A65
I
3',3'-cGAMP
A64
A56
U55
A65
G68
G69
A8
A9
J
U55
A9
K
A64
U32
L
G68
A65

Figure 1

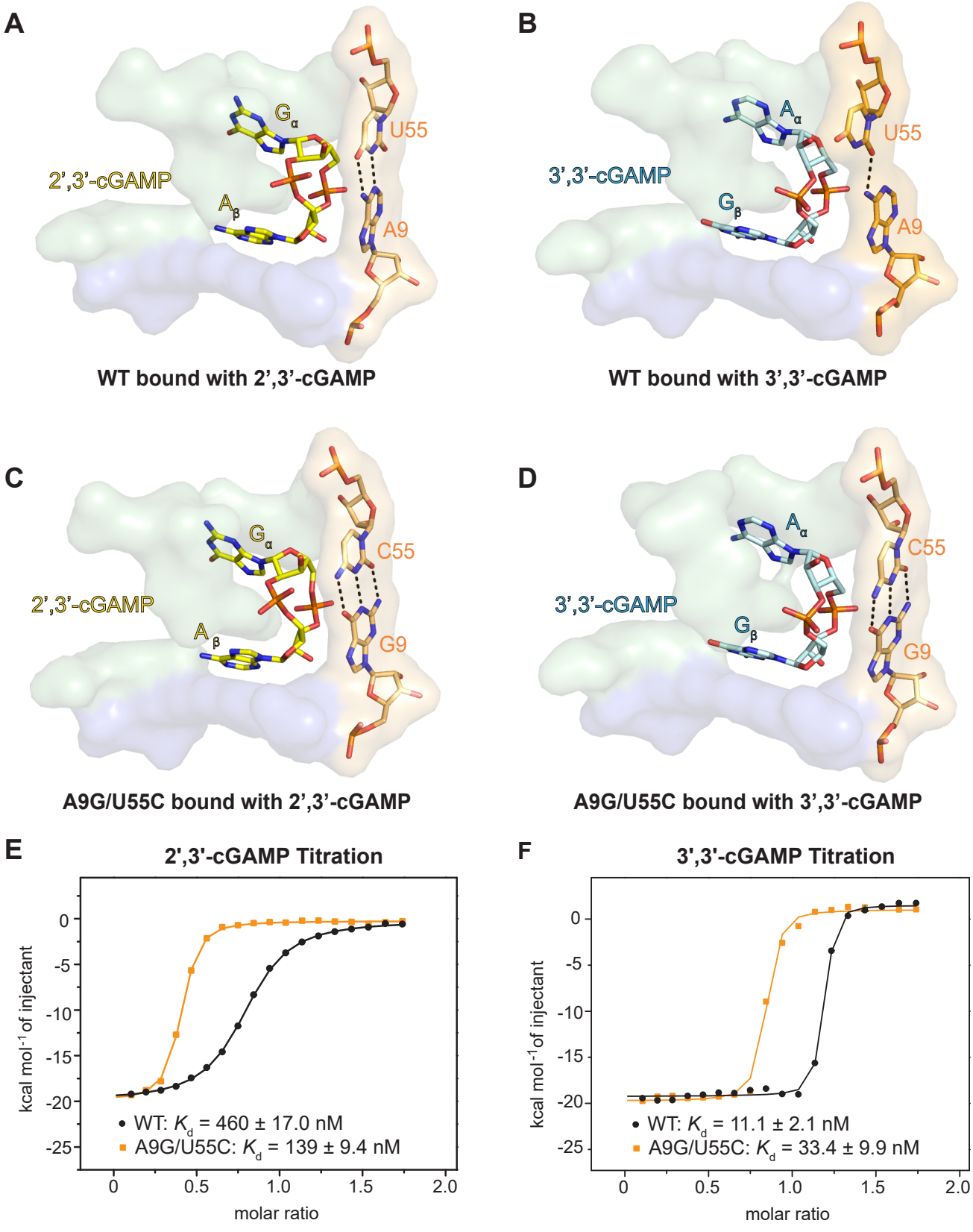
A
2',3'-cGAMP
G
α
A
β
U55
A9
WT bound with 2',3'-cGAMP
B
3',3'-cGAMP
A
α
G
β
U55
A9
WT bound with 3',3'-cGAMP
C
2',3'-cGAMP
G
α
A
β
C55
G9
A9G/U55C bound with 2',3'-cGAMP
D
3',3'-cGAMP
A
α
G
β
C55
G9
A9G/U55C bound with 3',3'-cGAMP
E
2',3'-cGAMP Titration
kcal mol-1 of injectant
0
-5
-10
-15
-20
-25
0
0.5
1.0
1.5
2.0
molar ratio
WT: Kd = 460 ± 17.0 nM
A9G/U55C: Kd = 139 ± 9.4 nM
F
3',3'-cGAMP Titration
kcal mol-1 of injectant
molar ratio
WT: Kd = 11.1 ± 2.1 nM
A9G/U55C: Kd = 33.4 ± 9.9 nM

Figure 2